Computations of Magnetic Resonance Parameters for Crystalline Systems: Principles

Jonathan R. Yates
University of Cambridge, Cambridge, UK
&
Chris J. Pickard
University of St. Andrews, St. Andrews, UK

1 INTRODUCTION

Magnetic resonance experiments of increasing sophistication probe the structure and dynamics of solid-state materials, for example, to determine the arrangement of atoms in a lattice, the packing of units in a molecular crystal, or the structure of a defect site. There is a clear need for quantitative theoretical support for these experiments, particularly to link the observed spectrum to the underlying microscopic structure. First-principles quantum-mechanical methods have the potential to provide this information. Indeed, traditional quantum-mechanical techniques have long been used to study isolated molecules and establish important links between structure and spectra (see ***Shielding Calculations***). However, when one is interested in the magnetic response of extended systems, it is important to take into account the crystal nature of the material; attempts to extend quantum chemical approaches have been made, for example, by representing the effects of the crystal lattice through an arrangement of point charges, or by constructing an appropriately sized cluster of atoms or molecules. However, an alternative approach is to start from common material modeling techniques which exploit the translation symmetry inherent in crystals. The first of these was the use of the linear augmented plane wave (LAPW) approach to compute electric field gradients (EFGs). More recently, there has been a series of developments based on the planewave-pseudopotential technique and it is now possible to compute NMR chemical shifts and J-couplings, as well as electron paramagnetic resonance (EPR) g-tensors and hyperfine couplings, for crystalline systems.

2 OVERVIEW OF THE PLANEWAVE-PSEUDOPOTENTIAL APPROACH

There are numerous first-principles methods applicable to either molecules or solid-state systems. The following section outlines the planewave-pseudopotential technique that has proved to be a useful platform for the prediction of solid-state magnetic resonance parameters. Further details can be found in the book by Martin[1] or in the review of Payne *et al.*[2]

2.1 Density Functional Theory

The behavior of a collection of electrons and nuclei can be predicted by solving the Schrödinger equation for the system:

$$\hat{H}\Psi = E\Psi \tag{1}$$

where the Hamiltonian $\hat{H}$ describes the various electrostatic interactions between the particles. An important simplification can be made by noting that the mass of the nuclei is much greater than the electron mass. This leads to the Born-Oppenheimer approximation, in which the electronic and nuclear degrees of freedom can be separated. Even with this simplification, it is still impractical to solve equation (1) for anything other than the most trivial system. The difficulty lies in its many-body nature—the fact that the electronic degrees of freedom are coupled to each other.

The Kohn–Sham formulation of density functional theory (DFT) treats the electronic charge density ρ as the fundamental variable and exactly maps the many-body equation (1) onto a set of N equations involving single-particle wavefunctions,

$$-\frac{\hbar^2}{2m_e}\nabla^2\Psi(\mathbf{r}) + v_{\text{eff}}(\mathbf{r})\Psi(\mathbf{r}) = \varepsilon\Psi(\mathbf{r}) \tag{2}$$

where the Kohn–Sham potential, $v_{\text{eff}}(\mathbf{r})$ contains terms arising from the interaction with the ionic charges $V_{\text{ion}}(\mathbf{r})$, the Coulomb interaction energy of the charge density interacting with itself (known as the *Hartree energy*), and a potential V_{xc}, which describes the effects of exchange and correlation between the electrons:

$$v_{\text{eff}}(\mathbf{r}) = V_{\text{ion}}(\mathbf{r}) + \int \mathrm{d}\mathbf{r}' \frac{\rho(\mathbf{r}')}{|\mathbf{r}-\mathbf{r}'|} + V_{\text{xc}}[\rho(\mathbf{r})] \tag{3}$$

The set of independent particle equations (2) and (3) are amenable to computation, but at the price that the form of the potential V_{xc} is unknown. It is necessary to make physically motivated approximations in order to make progress. Fortunately, simple approximations have been shown to be adequate for many purposes. In solid-state studies, the most simple useful approximation is the local density approximation (LDA) in which the exchange-correlation energy at a given point is taken to be the same as in a uniform electron gas with the same charge density. For many properties, adding terms dependent on the gradient of the density (the generalized gradient approximation, GGA) provides an improvement. Numerous GGAs have been proposed; the one by Perdew, Burke, and Ernzerhof[3] (PBE) has been used for many solid-state NMR

calculations. In quantum-chemical calculations based on localized orbital basis sets, it is common to use hybrid functionals, which include a proportion of Hartree–Fock exchange. In an extended basis, such as planewaves, hybrid functionals have a high computational cost. While hybrid functionals have been used to compute the ground-state structures of crystals, they have not yet been applied for the calculation of NMR chemical shifts in solids.

2.2 Bloch's Theorem

For any realistic crystal, the total number of electrons is vast. It is naturally desirable to exploit the translational symmetry of a crystalline material and consider only the crystallographic unit cell under periodic boundary conditions. That this is possible follows from Bloch's theorem:[a] As the potential has lattice periodicity (i.e., $v_{\text{eff}}(\mathbf{r}) = v_{\text{eff}}(\mathbf{r} + \mathbf{R})$ for all $\mathbf{R}$ where $\mathbf{R}$ is a lattice vector), then the eigenstates of the single-particle Hamiltonian can be written as

$$\Psi_{n,\mathbf{k}}(\mathbf{r}) = \mathrm{e}^{\mathrm{i}\mathbf{k}.\mathbf{r}} u_{n,\mathbf{k}}(\mathbf{r}) \tag{4}$$

where $u_{n,\mathbf{k}}$ is a function periodic in the unit cell such that $u_{n,\mathbf{k}}(\mathbf{r}) = u_{n,\mathbf{k}}(\mathbf{r} + \mathbf{R})$ for all lattice vectors $\mathbf{R}$. These Bloch states are labeled by their crystal momentum $\mathbf{k}$. The only unique values of $\mathbf{k}$ lie within the reciprocal unit cell, or equivalently and by convention, within the first Brillouin Zone (i.e., the Wigner–Seitz cell of the reciprocal lattice).

The problem of solving for an infinite number of electrons has become one of calculating for a finite number of bands at an infinite number of $\mathbf{k}$-points. However, physical properties are expected to smoothly vary with $\mathbf{k}$ and hence many integrals can be well approximated by a finite sampling of $\mathbf{k}$. A common scheme for Brillouin zone integration consists of the sets of regular integration grids introduced by Monkhorst and Pack.[4]

2.3 The Supercell Approximation

The application of periodic boundary conditions forces periodicity on the system studied. To address systems that do not have full three-dimensional translational symmetry—for example, in the study of disordered systems, defects, impurities, or the interaction of molecules and surfaces, the so-called supercell approximation can be used. Aperiodic systems are approximated by enclosing the region of interest in either bulk material (for a defect) or vacuum (for a molecule) and then periodically repeating this cell throughout space (Figure 1). The supercell must be large enough for the fictitious interactions between neighboring cells to be negligible.

2.4 The Planewave Basis Set

In order to solve the eigenvalue problem of equation (2) numerically, the eigenstates must be represented by some basis set. While there are many possible choices, the one made here is to use planewaves as the basis. There are many advantages in the use of planewaves: they form a mathematically simple basis, they naturally incorporate periodic boundary conditions, and, perhaps most importantly, planewave calculations can be

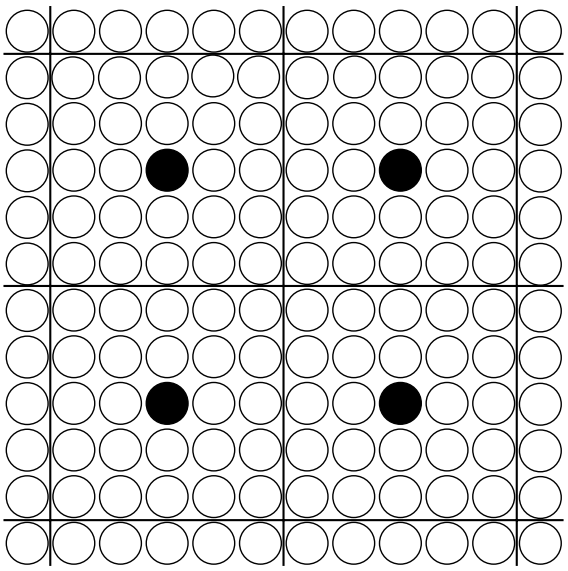

Figure 1 The supercell approximation: modeling a point defect within periodic boundary conditions

taken systematically to convergence as a function of the size of the basis. The Kohn–Sham eigenstates are expressed as

$$\Psi_{n,\mathbf{k}}(\mathbf{r}) = \sum_{\mathbf{G}} c_{n,\mathbf{k}}(\mathbf{G}) \mathrm{e}^{\mathrm{i}(\mathbf{k}+\mathbf{G}).\mathbf{r}} \tag{5}$$

where the sum is over all reciprocal lattice vectors $\mathbf{G}$. $c_{n,\mathbf{k}}(\mathbf{G})$ are the coefficients to be determined in solving equation (2). To truncate the basis set, the sum is limited to a set of reciprocal lattice vectors contained within a sphere with a radius defined by the cutoff energy, E_{cut}:

$$\frac{\hbar^2 |\mathbf{k} + \mathbf{G}|^2}{2m} \leq E_{\text{cut}} \tag{6}$$

Hence, the basis set is defined by the maximum kinetic energy component it contains. Physical quantities can be converged systematically by increasing E_{cut}. A fast-fourier transform (FFT) can be used to change the representation of the eigenstates from a sum of Fourier components to a uniform grid of points in the real-space unit cell. The use of numerically efficient FFTs is one key to the success of the planewave-pseudopotential formalism—it allows individual operations to be performed in the most efficient basis, e.g., the kinetic energy operator in Fourier space, and a local potential in real space.

2.5 The Pseudopotential Approximation

The electrons in an atom can be divided into two types—core electrons and valence electrons. The core electrons are tightly bound to the nucleus, while the valence electrons are more extended. A working definition for core electrons is that they are the ones that play no part in the interactions between atoms, while the valence electrons dictate most of the properties of the material. It is common to make the frozen core approximation; the core electrons are constrained not to differ from their free atomic nature when

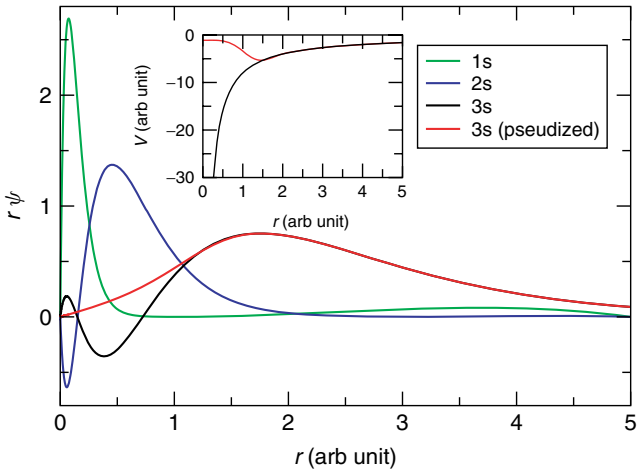

Figure 2 Si atomic orbitals: all-electron 1s, 2s, and 3s and the 3s pseudized orbital. Inset: all-electron potential and the corresponding potential felt by the pseudized 3s state

placed in the solid-state environment. This reduces the number of electronic degrees of freedom in an all-electron calculation. It is a very good approximation. A different, but physically related, approach is taken in the pseudopotential approximation. Since, in an all-electron calculation, the valence electron wavefunctions must be orthogonal to the core wavefunctions they necessarily have strong oscillations in the region near the nucleus (see the all-electron wavefunction in Figure 2). Given that a planewave basis set is to be used to describe the wavefunctions, these strong oscillations are undesirable—requiring many planewaves for an accurate description. Further, these oscillations are of very little consequence for the electronic structure in the solid, since they occur close to the nucleus. In the pseudopotential approach, only the valence electrons are explicitly considered, the effects of the core electrons being integrated within a new ionic potential. The valence wavefunctions need no longer be orthogonal to the core states, and so the orthogonality oscillations disappear; hence, far fewer planewaves are required to describe the valence wavefunctions. Numerous schemes to produce optimally soft pseudopotentials have been developed. Common choices are the norm-conserving potentials due to Troullier and Martins[5] and Vanderbilt's ultrasoft scheme.[6]

3 SHIELDING IN A PERIODIC SYSTEM

When a sample of matter is placed in a uniform external magnetic field electronic currents flow throughout the material. For an insulating nonmagnetic material, only the orbital motion of the electrons contribute to this current. The current density $\mathbf{j}(\mathbf{r})$, produces a nonuniform induced magnetic field in the material, which is given by the Biot–Savart law as

$$\mathbf{B}_{\text{in}}(\mathbf{r}) = \frac{\mu_0}{4\pi}\int \mathrm{d}^3 r' \mathbf{j}(\mathbf{r}') \times \frac{\mathbf{r}-\mathbf{r}'}{|\mathbf{r}-\mathbf{r}'|^3} \tag{7}$$

(note that we have used SI units throughout this article, which accounts for the different constants in these equations as compared to those in the original papers). The magnetic shielding tensor is defined as the ratio between this induced field and the external applied field

$$\mathbf{B}_{\text{in}}(\mathbf{r}) = -\boldsymbol{\sigma}(\mathbf{r})\mathbf{B}_{\text{ext}} \tag{8}$$

It is clear that the question of computing the shielding tensor is that of computing the induced electronic current. As the magnetic fields used in NMR experiments are small (in the sense that the corresponding Zeeman energy is a small term in the Hamiltonian), we can compute the induced current within perturbation theory, keeping quantities to linear order in the external field (we represent such linear quantities by a superscript (1)). To linear order, the current is given by

$$\mathbf{j}^{(1)}(\mathbf{r}') = 2\sum_o \left[\langle\Psi_o^{(0)}|\mathbf{J}^{\text{p}}(\mathbf{r}')|\Psi_o^{(1)}\rangle + \langle\Psi_o^{(1)}|\mathbf{J}^{\text{p}}(\mathbf{r}')|\Psi_o^{(0)}\rangle\right] + 2\sum_o \langle\Psi_o^{(0)}|\mathbf{J}^{\text{d}}(\mathbf{r}')|\Psi_o^{(0)}\rangle \tag{9}$$

where the factor of 2 accounts for spin degeneracy and the current operator, $\mathbf{J}(\mathbf{r}')$, has been written as the sum of diamagnetic and paramagnetic terms,

$$\mathbf{J}(\mathbf{r}') = \mathbf{J}^{\text{d}}(\mathbf{r}') + \mathbf{J}^{\text{p}}(\mathbf{r}') \tag{10}$$

$$\mathbf{J}^{\text{d}}(\mathbf{r}') = \frac{e^2}{m_e}\mathbf{A}(\mathbf{r}')|\mathbf{r}'\rangle\langle\mathbf{r}'| \tag{11}$$

$$\mathbf{J}^{\text{p}}(\mathbf{r}') = -\frac{e}{2m_e}\mathbf{p}|\mathbf{r}'\rangle\langle\mathbf{r}'| + |\mathbf{r}'\rangle\langle\mathbf{r}'|\mathbf{p} \tag{12}$$

Within perturbation theory, $|\Psi_o^{(1)}\rangle$ is given by

$$|\Psi_o^{(1)}\rangle = \sum_e \frac{|\Psi_e^{(0)}\rangle\langle\Psi_e^{(0)}|}{\varepsilon-\varepsilon_e}H^{(1)}|\Psi_o^{(0)}\rangle = \mathcal{G}(\varepsilon_o^{(0)})H^{(1)}|\Psi_o^{(0)}\rangle \tag{13}$$

where the Green function $\mathcal{G}(\varepsilon_o^{(0)})$ has been introduced. Using the symmetric gauge for the vector potential, $\mathbf{A}(\mathbf{r}) = 1/2\mathbf{B}\times\mathbf{r}$, the linear-order Hamiltonian is given by $H^{(1)} = e/m_e\mathbf{A}\cdot\mathbf{p}$ and we arrive at the following expression for the induced current,

$$\mathbf{j}^{(1)}(\mathbf{r}') = \frac{4e}{m_e}\sum_o \mathrm{Re}\left[\langle\Psi_o^{(0)}|\mathbf{J}^{\text{p}}(\mathbf{r}')\mathcal{G}(\varepsilon_o^{(0)})\mathbf{r}\times\mathbf{p}|\Psi_o^{(0)}\rangle\right]\cdot\mathbf{B} - \frac{e^2}{2m_e}\rho(\mathbf{r}')\mathbf{B}\times\mathbf{r}' \tag{14}$$

where $\rho(\mathbf{r}') = 2\sum_o\langle\Psi_o^{(0)}|\mathbf{r}'\rangle\langle\mathbf{r}'|\Psi_o^{(0)}\rangle$ is the ground-state charge density. So far, no distinction between finite and extended systems has been made. In the following sections, the conceptual and practical difficulties in applying equation (14) to extended systems are discussed.

3.1 The Position Operator Problem

For a finite system there is, in principle, no problem in computing the induced current directly from equation (14). However, for an extended system, there is an obvious problem with the second (diamagnetic) term of equation (14); the

presence of the position operator, $\mathbf{r}$, will generate a large contribution far away from $\mathbf{r} = 0$, and the term will diverge in an infinite system. The situation is saved by recognizing that an equal but opposite divergence occurs in the first (paramagnetic) term of equation (14), and so only the sum of the two terms is well defined. Through the use of a sum rule, we arrive at an alternative expression for the current

$$\mathbf{j}^{(1)}(\mathbf{r}') = \frac{4e}{m_e}\sum_o \mathrm{Re}\left[\langle\Psi_o^{(0)}|\mathbf{J}^{\mathrm{p}}(\mathbf{r}')\mathcal{G}(\varepsilon_o^{(0)})(\mathbf{r}-\mathbf{r}')\times\mathbf{p}|\Psi_o^{(0)}\rangle\right]\cdot\mathbf{B} \tag{15}$$

In an insulator the Green function $\mathcal{G}(\varepsilon_o^{(0)})$ is localized and so $\mathbf{j}^{(1)}(\mathbf{r}')$ remains finite at large values of $(\mathbf{r}-\mathbf{r}')$.

At this point, there still remains the question of the practical computation of the current, which for reasons of efficiency, it is desirable to work with just the part of the Bloch function, which is periodic in the unit cell ($u_{n,\mathbf{k}}$ in equation 4). Equation (15) is not suitable for such a calculation as the position operator does not have the periodicity of the unit cell. One solution to this problem is to consider the response to a magnetic field with a finite wavelength, q. In the limit that $q \to 0$, the uniform field result is recovered. For a practical calculation, this enables one to work with the $u_{n,\mathbf{k}}$, at the cost that a calculation at a point in the Brillouin Zone $\mathbf{k}$ will require knowledge of the wavefunctions at $\mathbf{k} \pm \mathbf{q}$ (i.e., six extra calculations for the full tensor). A complete derivation was presented in Refs. 7, 8 leading to the final result for the current,

$$\mathbf{j}^{(1)}(\mathbf{r}') = \lim_{q\to 0}\frac{1}{2q}\left[\mathbf{S}(\mathbf{r}',q)-\mathbf{S}(\mathbf{r}',-q)\right] \tag{16}$$

where

$$\mathbf{S}(\mathbf{r}',q) = \frac{2e}{m_e N_{\mathrm{k}}}\sum_{i=x,y,z}\sum_{o,\mathbf{k}}\mathrm{Re}\left[\frac{1}{i}\right.$$
$$\left.\times\langle u_{o,\mathbf{k}}^{(0)}|\mathbf{J}^{\mathrm{p}}_{\mathbf{k},\mathbf{k}+\mathbf{q}_i}(\mathbf{r}')\mathcal{G}_{\mathbf{k}+\mathbf{q}_i}(\varepsilon_{o,\mathbf{k}})\mathbf{B}\times\hat{\mathbf{u}}_i\cdot(\mathbf{p}+\mathbf{k})|u_{o,\mathbf{k}}^{(0)}\rangle\right] \tag{17}$$

$\mathbf{q}_i = q\hat{\mathbf{u}}_i$, N_{k} is the number of $\mathbf{k}$-points included in the summation and

$$\mathbf{J}^{\mathrm{p}}_{\mathbf{k},\mathbf{k}+\mathbf{q}_i} = -\frac{e}{2m_e}(\mathbf{p}+\mathbf{k})|\mathbf{r}'\rangle\langle\mathbf{r}'| + |\mathbf{r}'\rangle\langle\mathbf{r}'|(\mathbf{p}+\mathbf{k}+\mathbf{q}_i) \tag{18}$$

An alternative solution to this problem was developed by Sebastiani.[9] Rather than compute the magnetic response using extended Bloch functions, a transformation to Wannier orbitals is made. As Wannier orbitals can be chosen to be well localized around a particular lattice site, it is then possible to apply equation (15) directly, using a position operator in the form of a saw-tooth function.

When a planewave basis set is used, $\mathbf{j}^{(1)}(\mathbf{r}')$ will be obtained on the points of the FFT grid. In general, these will not coincide with the positions of the nuclei, and so to compute the induced field, $\mathbf{B}^{(1)}(\mathbf{R})$, equation (7) and $\mathbf{j}^{(1)}(\mathbf{r}')$ are Fourier transformed into reciprocal space. The induced magnetic field can then be simply evaluated as

$$\mathbf{B}^{(1)}(\mathbf{G}) = \mu_0\frac{i\mathbf{G}\times\mathbf{j}^{(1)}(\mathbf{G})}{G^2} \tag{19}$$

where $\mathbf{G}$ is a reciprocal lattice vector. $\mathbf{B}^{(1)}(\mathbf{R})$ is subsequently obtained by a explicit Fourier transform at the nuclear positions $\mathbf{R}$

$$\mathbf{B}^{(1)}(\mathbf{R}) = \sum_{\mathbf{G}} e^{i\mathbf{G}\cdot\mathbf{R}}\mathbf{B}^{(1)}(\mathbf{G}) \tag{20}$$

The computational work in evaluating this Fourier transform is very much smaller than that needed to obtain $\mathbf{j}^{(1)}(\mathbf{r}')$. As such, the cost of obtaining the shielding at a single atomic site is essentially identical to evaluating it at all atomic sites. Taking this further, it is also straightforward to obtain the shielding on an arbitrary set of points—the so-called nucleus independent chemical shift (NICS) or to make a map of the flow of the induced current; see Figure 3.

For $\mathbf{G} = 0$, equation (19) cannot be applied. Indeed the $\mathbf{G} = 0$ component of the induced magnetic field is not a bulk property;[10] rather it is determined by the induced currents on the surface of the sample. In particular, its value depends on the shape of the sample, and is determined by macroscopic magnetostatics (see ***Magnetic Susceptibility and High Resolution NMR of Liquids and Solids***). In order to compare with results from MAS experiments, a spherical sample should be assumed for which

$$\mathbf{B}^{(1)}(\mathbf{G}=\mathbf{0}) = \frac{2\mu_0}{3}\overleftrightarrow{\chi}\mathbf{B} \tag{21}$$

where $\overleftrightarrow{\chi}$ is the macroscopic magnetic susceptibility. $\overleftrightarrow{\chi}$ is directly provided by first-principles calculation, and can be used to adjust the shieldings for arbitrary sample shapes, should this be required.

Finally, we note that experiments typically measure the change in shielding relative to a reference standard—the chemical shift δ. The conversion is straightforward

$$\delta = -[\sigma - \sigma_{\mathrm{ref}}^{\mathrm{iso}}] \tag{22}$$

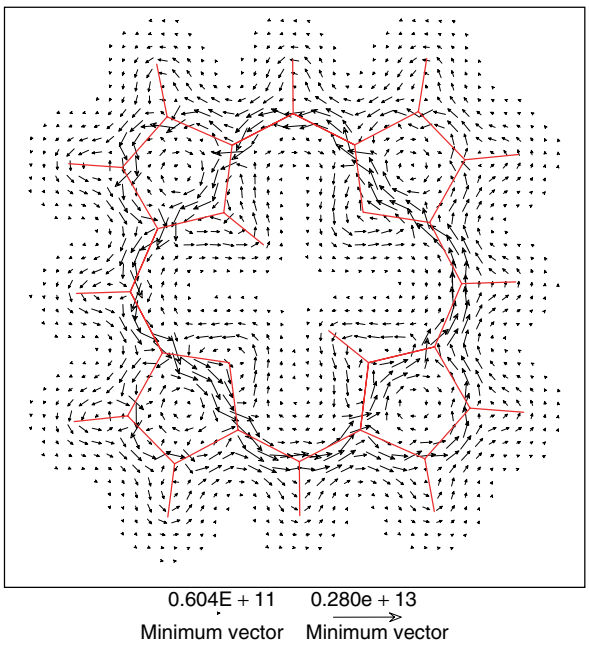

Figure 3 Current flow in porphyrin. Height above molecular plane is 0.53 (Bohr). Vectors are scaled such that minimum: 0.6 × $10^{11} nAT^{-1}Bohr^{-2}$, maximum: 0.3 × $10^{13} nAT^{-1}Bohr^{-2}$

The shielding of the reference standard, $\sigma_{\text{ref}}^{\text{iso}}$, could be obtained by performing a calculation on the standard compound itself, but this is often not convenient—for example, if the reference is a liquid or solution. For this reason, most studies have obtained $\sigma_{\text{ref}}^{\text{iso}}$ as the intercept of a line of unit gradient fitted to a graph of calculated shieldings against experimental shifts.

3.2 Core States and Pseudopotentials

In the planewave-pseudopotential approach, it is implicit that the core electrons can be treated separately from the valence states in an atomic code. Historically, the validity of the frozen core approximation for NMR properties had been doubted, but a careful study by Gregor, Mauri, and Car[11] showed that, if the core and valence states are partitioned in a gauge-invariant way, the shielding of the core electrons is chemically insensitive. The contribution of the core electrons to chemical shifts can hence be neglected. If absolute shieldings are required, the core contribution is most conveniently calculated by setting the gauge origin at the atomic center, so that the shielding is purely diamagnetic and given by the Lamb formula,

$$\sigma_{ij} = \delta_{ij} \frac{\mu_0 e^2}{4\pi m_e} \int \mathrm{d}^3 r \frac{n(\mathbf{r})}{r} \tag{23}$$

As shown in Figure 2, the use of pseudopotentials implies a nonphysical form for the wavefunction in the region close to the nucleus. For this reason, a formalism based on pseudopotentials might appear a poor choice for the calculation of *nuclear* magnetic resonance parameters. The upper part of Figure 4 shows shieldings computed for a range of isolated molecules by using only the pseudowavefunctions (i.e., neglecting the fact that the pseudowavefunction differs from the true all-electron wavefunction close to the nucleus), and the corresponding large basis set quantum-chemical calculations. For proton shieldings, the agreement is reasonable. For ^{13}C, the pseudopotential results reproduce the general trend of the all-electron shieldings although the slope is somewhat less than unity. Uncorrected pseudopotential calculations for proton and first row elements have been presented (see e.g., Ref. 12); the agreement can be improved by using rather hard pseudopotentials (i.e., a small matching radius). For the second row elements, Si and P, Figure 4 shows the impact of the pseudopotential approximation to be dramatic with almost all of the chemical sensitivity lost. In order to make direct comparison to experiment, it is therefore vital to correctly account for the use of pseudopotentials and to obtain shieldings with the accuracy of all-electron calculations.

The basis for such an approach was provided by projector augmented wave (PAW) method introduced by van de Walle and Blöchl.[14] In this scheme, a linear transformation $\mathcal{T}$ maps the valence pseudo wavefunctions $|\tilde{\Psi}\rangle$ onto the corresponding all-electron wavefunctions, $|\Psi\rangle = \mathcal{T}|\tilde{\Psi}\rangle$,

$$\mathcal{T} = \mathbf{1} + \sum_{\mathbf{R},n} [|\phi_{\mathbf{R},n}\rangle - |\tilde{\phi}_{\mathbf{R},n}\rangle]\langle \tilde{p}_{\mathbf{R},n}| \tag{24}$$

$|\phi_{\mathbf{R},n}\rangle$ are all-electron atomiclike states obtained from a calculation on an isolated atom and $|\tilde{\phi}_{\mathbf{R},n}\rangle$ are the corresponding pseudized states. $\langle \tilde{p}_{\mathbf{R},n}|$ are a set of projectors such that $\langle \tilde{p}_{\mathbf{R},n}|\tilde{\phi}_{\mathbf{R}',m}\rangle = \delta_{\mathbf{R},\mathbf{R}'}\delta_{n,m}$. $\mathbf{R}$ labels the atomic site

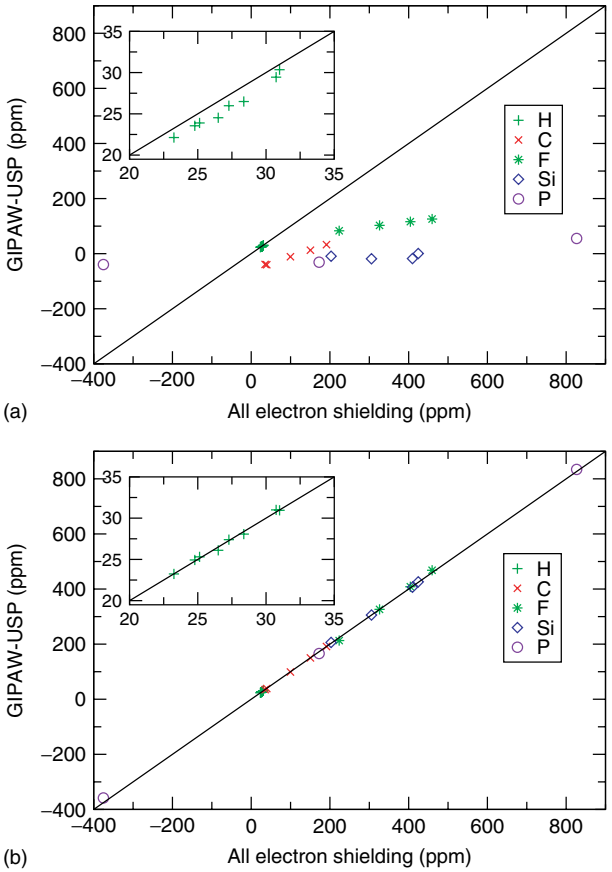

Figure 4 Isotropic magnetic shielding for nuclear sites in a range of molecules. The graphs show shieldings obtained by the GIPAW method and ultrasoft pseudopotentials plotted against all-electron shielding. The straight line represents perfect agreement. The upper figure (a) shows the contribution without GIPAW augmentation, the lower figure (b) plots the total contribution. (Reproduced from Ref. 13. © American Physical Society, 2007)

and n is a composite index that accounts for the angular momentum and the number of projectors. In simple terms, the PAW transformation works by computing the component of a certain atomic-like state (say 2p) in a pseudowavefunction, and replacing the pseudized component by its all-electron form. This may seem like a rather approximate procedure, but because the atomic states form a good basis for the wavefunction in the region close to the nucleus, it can be made highly accurate by using multiple projectors.

Within the PAW scheme, for an all-electron local or semilocal operator O, the corresponding pseudooperator, $\widetilde{O}$, is given by

$$\widetilde{O} = O + \sum_{\mathbf{R},n,m} |\tilde{p}_{\mathbf{R},n}\rangle \big[\langle \phi_{\mathbf{R},n}|O|\phi_{\mathbf{R},m}\rangle - \langle \tilde{\phi}_{\mathbf{R},n}|O|\tilde{\phi}_{\mathbf{R},m}\rangle\big]\langle \tilde{p}_{\mathbf{R},m}| \tag{25}$$

As constructed in equation (25), the pseudooperator $\widetilde{O}$ acting on pseudowavefunctions will give the same matrix elements as the all-electron operator O acting on all-electron wavefunctions.

For a system under a uniform magnetic field, PAW alone is not a computationally realistic solution. In using a set of

localized functions, the gauge-origin problem, well known in quantum chemical approaches (see ***Shielding: Overview of Theoretical Methods***), has been introduced. In short, equation (25) will require an infinitely large number of projectors in order for the computed shieldings to be translationally invariant (i.e., independent of the choice of gauge origin). To address this problem, Pickard and Mauri[8] introduced a field-dependent transformation operator $\mathcal{T}_{\mathbf{B}}$, which, by construction, imposes the translational invariance exactly:

$$\mathcal{T}_{\mathbf{B}} = \mathbf{1} + \sum_{\mathbf{R},n} e^{\frac{ie}{2\hbar}\mathbf{r}\cdot\mathbf{R}\times\mathbf{B}}[|\phi_{\mathbf{R},n}\rangle - |\tilde{\phi}_{\mathbf{R},n}\rangle]\langle\tilde{p}_{\mathbf{R},n}|e^{-\frac{ie}{2\hbar}\mathbf{r}\cdot\mathbf{R}\times\mathbf{B}} \quad (26)$$

The resulting approach is known as the *gauge including projector augmented wave* (*GIPAW*) method. Although originally formulated for norm-conserving pseudopotentials, the extension to the more computationally efficient ultrasoft pseudopotentials has been presented by Yates *et al*.[13] Figure 4 shows shieldings computed using ultrasoft pseudopotentials and the GIPAW scheme, together with large basis set quantum-chemical calculations. For the shieldings in these isolated molecules, the agreement is essentially perfect. For crystalline systems, validation of the technique comes only from comparison to NMR experiments; numerous studies have been made in recent years, just two are mentioned in section "Examples".

4 OTHER MAGNETIC RESONANCE PARAMETERS

4.1 Electric Field Gradient

For a quadrupolar nucleus (spin $I > 1/2$), the observed NMR response includes an interaction between the quadrupole moment of the nucleus Q, and the electric field gradient (EFG) generated by its surroundings. The EFG is a second rank, symmetric, traceless tensor $V(\mathbf{r})$ given by

$$V_{\alpha\beta}(\mathbf{r}) = \frac{\partial E_\alpha(\mathbf{r})}{\partial r_\beta} - \frac{1}{3}\delta_{\alpha\beta}\sum_\gamma \frac{\partial E_\gamma(\mathbf{r})}{\partial r_\gamma} \quad (27)$$

where α,β,γ denote the Cartesian coordinates x,y,z and $E_\alpha(\mathbf{r})$ is the local electric field at the position $\mathbf{r}$, which can be calculated from the charge density $n(\mathbf{r})$:

$$E_\alpha(\mathbf{r}) = \int \mathrm{d}^3 r \frac{n(\mathbf{r})}{|\mathbf{r}-\mathbf{r}'|^3}(r_\alpha - r'_\alpha) \quad (28)$$

The EFG tensor is then equal to

$$V_{\alpha\beta}(\mathbf{r}) = \int \mathrm{d}^3 r \frac{n(\mathbf{r})}{|\mathbf{r}-\mathbf{r}'|^3}\left[\delta_{\alpha\beta} - 3\frac{(r_\alpha - r'_\alpha)(r_\beta - r'_\beta)}{|\mathbf{r}-\mathbf{r}'|^2}\right] \quad (29)$$

To compute the EFG tensor in a periodic system is less demanding than calculating either the shielding or indirect coupling tensors, as it requires only knowledge of the ground-state charge density, ground-state wavefunctions and the position of the ions in the unit cell—no linear response calculation is required.

The quadrupolar coupling constant, C_Q and the asymmetry parameter, η_Q can be obtained from the diagonalized electric field gradient tensor whose eigenvalues are labeled V_{XX}, V_{YY}, V_{ZZ}, such that $|V_{ZZ}|>|V_{XX}|>|V_{YY}|$:

$$C_Q = \frac{eV_{ZZ}Q}{h} \quad (30)$$

and

$$\eta_Q = \frac{V_{YY} - V_{XX}}{V_{ZZ}} \quad (31)$$

Within the planewave-pseudopotential approach, the charge density is expressed as the sum of three terms,[15] and there are correspondingly three distinct contributions to the EFG. First, there is a contribution arising from the ionic charges (sum of the nuclear and core-electron charge). From the site under consideration, this appears as an infinite lattice of point charges whose EFG contribution can be obtained using an Ewald summation. Secondly, there is the contribution of the pseudized valence charge density, which is evaluated by using a reciprocal space form of equation (29). Finally, there is a PAW contribution to account for the difference between the pseudo and all-electron charge densities on the atomic site under consideration.

4.2 Indirect Coupling

The indirect (or J) coupling manifests itself in splittings of the NMR resonance, or as a modulation of the spin-echo signal. Physically, the coupling arises from the interaction of two nuclei, K and L, with magnetic moments, μ_K and μ_L, mediated by the electrons in the system. The first complete analysis of this indirect coupling was provided by Ramsey[16,17] who showed that the J-coupling tensor, $\overleftrightarrow{\mathbf{J}}_{KL}$, is obtained from the magnetic field induced at nucleus K due to the perturbative effect of nucleus L,

$$\mathbf{B}^{(1)}_{\mathrm{in}}(\mathbf{R}_K) = \frac{\hbar\gamma_K\gamma_L}{2\pi}\overleftrightarrow{\mathbf{J}}_{KL}\cdot\mu_L \quad (32)$$

where γ_K and γ_L are the gyromagnetic ratios of nuclei K and L. At the nonrelativistic level, two distinct mechanisms contribute to $\mathbf{B}^{(1)}_{\mathrm{in}}(\mathbf{R}_K)$. First, the nuclei interact via the electronic charge; the nucleus L induces an orbital current $\mathbf{j}^{(1)}(\mathbf{r})$ which, in turn, creates a magnetic field at nucleus K. The nuclei also interact via the electronic spin; the nucleus L inducing a polarization of the electronic spin, $\mathbf{m}^{(1)}(\mathbf{r})$, which also contributes to the magnetic field at nucleus K. $\mathbf{B}^{(1)}_{\mathrm{in}}(\mathbf{R}_K)$ is given by

$$\begin{aligned}\mathbf{B}^{(1)}_{\mathrm{in}}(\mathbf{R}_K) = {} & \frac{\mu_0}{4\pi}\int \mathbf{m}^{(1)}(\mathbf{r})\cdot\left[\frac{3\mathbf{r}_K\mathbf{r}_K - |\mathbf{r}_K|^2}{|\mathbf{r}_K|^5}\right]\mathrm{d}^3\mathbf{r} \\ & + \frac{\mu_0}{4\pi}\frac{8\pi}{3}\int \mathbf{m}^{(1)}(\mathbf{r})\delta(\mathbf{r}_K)\,\mathrm{d}^3\mathbf{r} \\ & + \frac{\mu_0}{4\pi}\int \mathbf{j}^{(1)}(\mathbf{r})\times\frac{\mathbf{r}_K}{|\mathbf{r}_K|^3}\,\mathrm{d}^3\mathbf{r}\end{aligned} \quad (33)$$

$\mathbf{r}_N = \mathbf{r} - \mathbf{R}_N$ with $\mathbf{R}_N$ the position of nucleus N; δ is the Dirac delta function.

The induced current can be computed using the equivalent expression for the shielding, equation (14), but using a vector potential of the form $\mathbf{A}(\mathbf{r}) = \frac{\mu_0}{4\pi}\frac{\mu_L \times \mathbf{r}_L}{|\mathbf{r}_L|^3}$. $\mathbf{m}^{(1)}(\mathbf{r})$ can also be computed through perturbation theory,

$$\mathbf{m}^{(1)}(\mathbf{r}) = g\beta\left[\mathbf{n}_{\uparrow}^{(1)}(\mathbf{r}) - \mathbf{n}_{\downarrow}^{(1)}(\mathbf{r})\right] = 2g\beta\mathbf{n}_{\uparrow}^{(1)}(\mathbf{r}) \tag{34}$$

with g the Lande g-factor and β the Bohr magneton. $\mathbf{n}_{\uparrow}^{(1)}(\mathbf{r})$ ($\mathbf{n}_{\downarrow}^{(1)}(\mathbf{r})$) is the spin up (down) charge density given by $\mathbf{n}_{\uparrow}^{(1)}(\mathbf{r}) = 2\sum_{occ} Re[\langle\Psi^{(0)}|\mathbf{r}\rangle\langle\mathbf{r}|\Psi_o^{(1)}\rangle]$. $|\Psi_o^{(1)}\rangle$ is given by

$$|\Psi_o^{(1)}\rangle = \sum_e \frac{|\Psi_e^{(0)}\rangle\langle\Psi_e^{(0)}|}{\varepsilon - \varepsilon_e} H_{\mathrm{M}}^{(1)}|\Psi_o^{(0)}\rangle = \mathcal{G}(\varepsilon_o^{(0)})H_{\mathrm{M}}^{(1)}|\Psi_o^{(0)}\rangle \tag{35}$$

with the first-order Hamiltonian given by the well-known Fermi-contact (FC) and spin-dipolar (SD) terms

$$H_{\mathrm{M}}^{(1)} = \mathrm{H_{FC}} + \mathrm{H_{SD}} \tag{36}$$

$$\mathrm{H_{FC}} = g\beta\frac{\mu_0}{4\pi}\frac{8\pi}{3}\mathbf{S}\cdot\mu_L\delta(\mathbf{r}_L) \tag{37}$$

$$\mathrm{H_{SD}} = g\beta\frac{\mu_0}{4\pi}\mathbf{S}\cdot\left(\frac{3\mathbf{r}_L(\mu_L\cdot\mathbf{r}_L) - r_L^2\mu_L\mathcal{I}}{|r_L|^5}\right) \tag{38}$$

where $\mathbf{S}$ is the Pauli spin operator and $\mathcal{I}$ the identity matrix. For analysis, it is common to divide the total J-coupling tensor into five components, although only the total tensor can be observed experimentally

$$\overleftrightarrow{\mathbf{J}}_{\mathrm{KL}} = \overleftrightarrow{\mathbf{J}}_{\mathrm{KL}}^{\mathrm{DSO}} + \overleftrightarrow{\mathbf{J}}_{\mathrm{KL}}^{\mathrm{PSO}} + \overleftrightarrow{\mathbf{J}}_{\mathrm{KL}}^{\mathrm{FC}} + \overleftrightarrow{\mathbf{J}}_{\mathrm{KL}}^{\mathrm{SD}} + \overleftrightarrow{\mathbf{J}}_{\mathrm{KL}}^{\mathrm{SD/FC}} \tag{39}$$

DSO and PSO refer, respectively, to the diamagnetic and paramagnetic-induced current response. The first four terms arise from symmetric interactions, with the same coupling mechanism at the perturbing and receiving sites. The term $\overleftrightarrow{\mathbf{J}}_{\mathrm{KL}}^{\mathrm{SD/FC}}$ is a cross term between the SD and FC interactions, which contributes only to the anisotropic part of $\overleftrightarrow{\mathbf{J}}_{\mathrm{KL}}$.

Joyce *et al.*[18] developed a technique to compute J-coupling tensors for solid-state systems using the planewave-pseudopotential formalism. PAW is used to provide all-electron accuracy; it is a strict test of the theory because the wavefunction reconstruction must be performed at both the perturbing and receiving nuclei.

Unlike the case of nuclear shielding, even for a truly periodic system, the J-coupling perturbation breaks the translational symmetry of the crystal, and a simulation supercell of sufficient size to inhibit the interaction of periodically repeated images of the perturbing site must be chosen. Often, the primitive crystallographic cell is large enough to give converged results; however, in some cases, it is necessary to consider a larger simulation cell containing two or more primitive cells. Initial results are promising; Table 1 shows computed and experimental ^{29}Si and ^{31}P NMR parameters for the silicophosphate $Si_5O(PO_4)_6$. Figure 5 highlights the two distinct coupling pathways between the P and Si_2 sites—the couplings are rather different in size and there is good agreement between experiment and calculation.

Table 1 Calculated NMR Chemical Shifts and J-Coupling for the Silicophosphate $Si_5O(PO_4)_6$. The Experimental Values are in Brackets. (Calculasions from Ref. 18, Experiment from Ref. 19)

Coupling	^{31}P (ppm)	^{29}Si (ppm)	$J^2_{\mathrm{P-O-Si}}$ (Hz)
$J^2_{\mathrm{P-O_3-Si_1}}$	−47.4 (−43.8)	−214.8 (−213.3)	−17.12 (15 ± 2)
$J^2_{\mathrm{P-O_2-Si_2}}$		−218.7 (−217.0)	−16.26 (14 ± 2)
$J^2_{\mathrm{P-O_5-Si_2}}$		−218.7 (−217.0)	−1.17 (4 ± 2)
$J^2_{\mathrm{P-O_4-Si_3}}$		−128.6 (−119.1)	−14.13 (12 ± 2)

4.3 Metallic Systems

The shielding in metallic systems arises from two mechanisms. The familiar orbital response of the electrons, outlined in section, "Shielding in a Periodic System" and the Knight shift, which arises from a spin polarization induced by the external field. d'Avezac *et al.*[20] have presented a planewave-pseudopotential approach to compute the shielding in metals. This uses GIPAW to compute the orbital response and PAW for the Knight shift. Chemical shifts for the elemental metals Al, Li, and Cu have been presented, showing good agreement with experiment. The calculations are somewhat more demanding than the equivalent calculation for insulators, because a very fine sampling of the Brillouin Zone is required.

4.4 EPR

In crystalline materials, EPR can be used to study paramagnetic defects. EPR spectra of spin 1/2 centers have two contributions: the hyperfine tensor $\mathbf{A}$ and the g-tensor $\mathbf{g}$, which are defined through the following effective Hamiltonian

$$H_{\mathrm{eff}} = \frac{\alpha}{2}\mathbf{S}\cdot\mathbf{g}\cdot\mathbf{B} + \sum_I \mathbf{S}\cdot\mathbf{A}_I\cdot\mathbf{I}_I \tag{40}$$

where α is the fine structure constant and the summation I runs over nuclei. The hyperfine tensor arises from the interaction of the nuclei with the ground-state spin density. This term has been calculated within the planewave-pseudopotential approach; indeed it was for this property that the PAW scheme was first introduced.[14] The g-tensor arises from the interaction of the electronic spin with the external magnetic field. This term plays a somewhat similar role to the shielding in NMR;

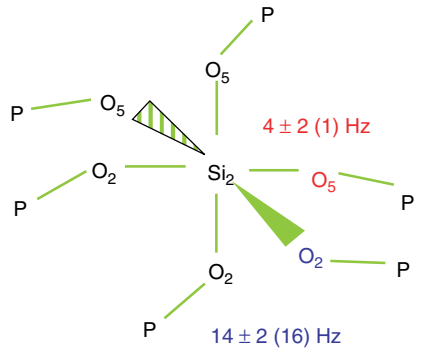

Figure 5 Schematic representation of the coupling pathways between Si_2 and P in $Si_5O(PO_4)_6$, showing the two experimental (calculated) J-couplings

induced electronic currents in the sample modify the g-tensor from its vacuum value. The GIPAW approach has been used to compute g-tensors in several crystalline materials,[21] including defects in α-quartz and zirconia.

4.5 Heavy Elements and Relativistic Effects

The Schrödinger equation is nonrelativistic; it is valid only for particles whose velocity is much smaller than the speed of light. This is a good approximation for electrons in materials comprising of light elements, but as we descend the periodic table relativistic effects begin to play an important role because both the low-lying core states, and the valence states in the region close to the nucleus obtain high values of momentum. Relativity has a significant effect on the bonding and structural properties of materials containing heavy elements, and unsurprisingly it also has a large influence on their magnetic resonance parameters. In treating such elements, it is therefore necessary to move to a description based on the Dirac equation, which is able to account for the influence of special relativity on the electronic states.

Numerous quantum-chemical approaches incorporating relativistic effects have been developed (see ***Relativistic Computation of NMR Shieldings and Spin-Spin Coupling Constants***). The use of pseudopotentials provides an alternative, simple, and computationally efficient route to including relativistic effects. In the initial construction of the pseudopotential, the free atom is treated relativistically, ensuring that the valence states have the correct relativistic eigenvalues. In the pseudopotential construction, it is usual to average over spin-orbit split states (the scalar-relativistic approximation), but it is possible to obtain pseudopotentials that include spin-orbit splitting. For bonding properties, it is sufficient to use only relativistic pseudopotentials; by construction, 'the pseudovalence wavefunctions have low momentum throughout space and can be treated nonrelativistically. For the calculation of properties with a large contribution in the region close to the nucleus, it is necessary to use PAW operators modified to account for relativistic effects. Yates *et al.*[22] have used GIPAW operators modified using the zeroth order regular approximation (ZORA) to compute ^{77}Se and ^{125}Te shieldings. Within this scheme, a relativistic calculation on TeH_2 has the same computational cost as a nonrelativistic calculation on OH_2.

5 EXAMPLES

The methods described in this article have been applied to a wide range of solid materials from molecular crystals (e.g., pharmaceutical polymorphs and amino acids) to inorganic solids such as silicate glasses and perovskites. Applications to molecular crystals are presented in the article by Harris *et al.* (see ***Chemical Shift Computations for Crystalline Molecular Systems: Applications***), here two illustrative examples are briefly mentioned.

Figure 6 shows a Heteronuclear Multiple Quantum Coherence (HMQC) spectra of the disaccharide maltose, in comparison with GIPAW calculations treating the system first as an isolated molecule and then as a full periodic crystal. The

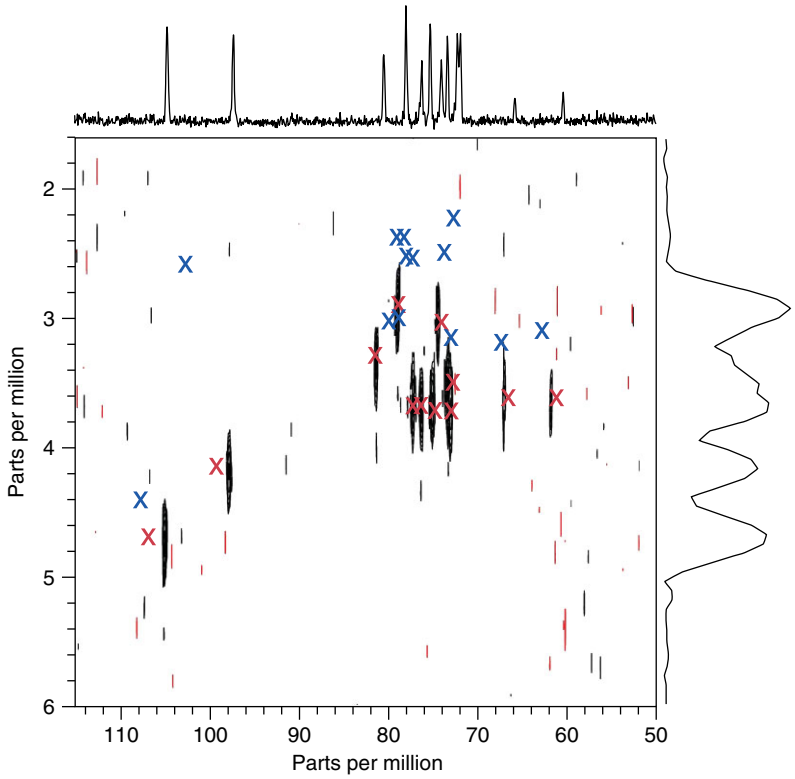

Figure 6 $^{13}C-^{1}H$ MAS J-HMQC solid-state NMR spectrum of maltose. The crosses show the positions of the peaks computed using the GIPAW method while treating the system as an isolated molecule (blue) and as a full crystal (red). (Reprinted with permission from Ref. 22. © (2005) American Chemical Society)

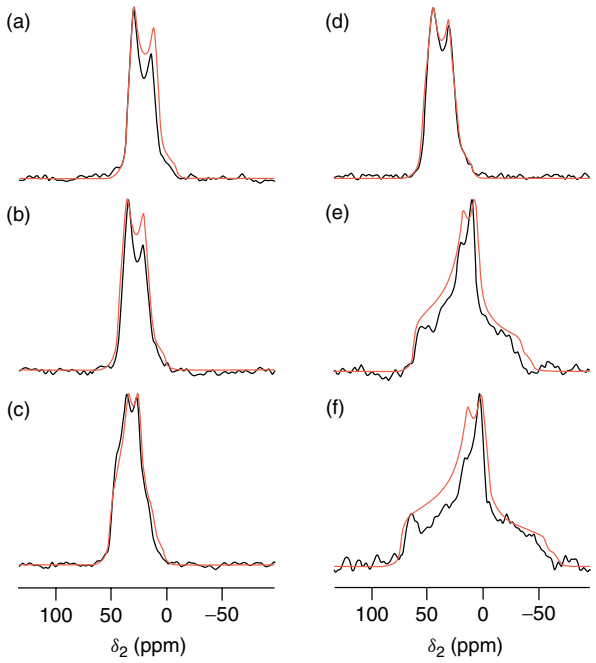

Figure 7 Cross-sections from the triple-quantum ^{17}O MAS spectrum of orthoenstatite. Shown in red are lineshapes simulated using NMR parameters computed using the GIPAW method. (Reprinted with permission from Ref. 23. © (2007) American Chemical Society)

excellent agreement between the crystalline calculation and experiment is sufficient to produce a full site assignment of the resonances. The significant differences between the isolated molecule and full crystal calculations show the importance of intramolecular interactions on the NMR parameters for this system. For maltose these changes have been shown to be due to the presence of so-called weak (C−H−O) hydrogen bonds.[23]

Figure 7 shows MAS line shapes extracted from an ^{17}O triple-quantum MAS spectrum of the $MgSiO_3$ polymorph orthoenstatite. These have characteristic quadrupolar lineshapes. In two cases, (b) and (c), the lineshape arises from the overlap of two resonances. Chemical shift and EFG tensors were computing using the planewave-pseudopotential approach, and the corresponding lineshapes, obtained using the calculated δ_{iso}, C_Q, and η_Q, are also shown in Figure 7. Again, the good agreement between theory and experiment allows a site assignment of the experimental resonances.[24]

End Note

[a]Named for Felix Bloch. This was result was derived by Bloch as part of his thesis work in 1928, long before his part in the history of NMR.

6 RELATED ARTICLES

Accurate Determination of Nuclear Quadrupole Coupling Constants and other NMR Parameters in Liquids from the Combination of Molecular Dynamics Simulations and ab initio Calculations; Shielding Tensor Calculations; Shielding Calculations; Relativistic Computation of NMR Shieldings and Spin-Spin Coupling Constants; Chemical Shift Computations for Crystalline Molecular Systems: Applications.

7 REFERENCES

1. R. M. Martin, *Electronic Structure: Basic Theory and Practical Methods*, CUP: Cambridge, 2004.
2. M. C. Payne, M. P. Teter, D. C. Allen, T. A. Arias, and J. D. Joannopoulos, *Rev. Mod. Phys.*, 1992, **64**, 1045.
3. J. P. Perdew, K. Burke, and M. Ernzerhof, *Phys. Rev. Lett.*, 1996, **77**, 3865.
4. H. J. Monkhorst and J. D. Pack, *Phys. Rev., B*, 1976, **13**, 5188.
5. N. Troullier and J. L. Martins, *Phys. Rev., B*, 1991, **43**, 1993.
6. D. Vanderbilt, *Phys. Rev., B*, 1990, **41**, 7892.
7. F. Mauri, B. G. Pfrommer, and S. G. Louie, *Phys. Rev. Lett.*, 1996, **77**, 5300.
8. C. J. Pickard and F. Mauri, *Phys. Rev., B*, 2001, **63**, 245101.
9. D. Sebastiani and M. Parrinello, *J. Phys. Chem. A*, 2001, **105**, 1951.
10. F. Mauri and S. G. Louie, *Phys. Rev. Lett.*, 1996, **76**, 4246.
11. T. Gregor, F. Mauri, and R. Car, *J. Chem. Phys.*, 1999, **111**, 1815.
12. D. Sebastiani, *Mod. Phys. Lett.*, 2003, **17**, 1301.
13. J. R. Yates, C. J. Pickard, and F. Mauri, *Phys. Rev., B*, 2007, **76**, 024401.
14. C. G. van de Walle and P. E. Blöchl, *Phys. Rev., B*, 1993, **47**, 4244.
15. M. Profeta, F. Mauri, and C. J. Pickard, *J. Am. Chem. Soc.*, 2003, **125**, 541.
16. N. F. Ramsey and E. M. Purcell, *Phys. Rev.*, 1952, **85**, 143.
17. N. F. Ramsey, *Phys. Rev.*, 1953, **91**, 303.
18. S. A. Joyce, J. R. Yates, C. J. Pickard, and F. Mauri, *J. Chem. Phys.*, 2007, **127**, 204107.
19. C. Coelho, T. Azaïs, L. Bonhomme-Coury, G. Laurent, and C. Bonhomme, *Inorg. Chem*, 2007, **46**, 1379.
20. M. d'Avezac, N. Marzari, and F. Mauri, *Phys. Rev., B*, 2007, **76**, 165122.
21. C. J. Pickard and F. Mauri, *Phys. Rev. Lett.*, 2002, **88**, 086403.
22. J. R. Yates, C. J. Pickard, M. C. Payne, and F. Mauri, *J. Chem. Phys.*, 2003, **118**, 5746.
23. J. R. Yates, T. N. Pham, C. J. Pickard, F. Mauri, A. M. Amado, A. M. Gil, and S. P. Brown, *J. Am. Chem. Soc.*, 2005, **127**, 10216.
24. S. E. Ashbrook, A. J. Berry, D. J. Frost, A. Gregorovic, C. J. Pickard, J. E. Readman, and S. Wimperis, *J. Am. Chem. Soc.*, 2007, **129**, 13213.

Biographical Sketches

Chris J. Pickard. b 1973. B.A. 1994, Ph.D., 1997 (supervisor Mike Payne), University of Cambridge, UK. Postdoctoral work in Taiwan, Germany, and Cambridge. Currently Reader in Physics, University of St Andrews. Approx. 80 papers. Research Interests: Computational electronic structure theory, core-level and magnetic resonance spectroscopy of solid-state systems. Crystal structure prediction.

Jonathan R. Yates. b 1977. M.Sci. 1999, Ph.D. 2003 (supervisor Mike Payne), University of Cambridge, UK. Postdoctoral work at University of California, Berkeley and Research Fellow Corpus Christi College, Cambridge. Currently Royal Society Research Fellow and University Lecturer, Department of Materials, University of Oxford. Approx. 20 papers. Research Interests: Computational electronic structure theory, particularly methods to predict magnetic resonance parameters for solid-state systems.